the
abdus salam
international
centre
for theoretical
physics

united nations educational, scientific and cultural organization

international atomic energy agency

preprint

NUMERICAL STUDY OF THE SPIN-1 ASHKIN-TELLER MODEL

S. Bekhechi

M. Badehdah

A. Benyoussef

and

B. Ettaki

IC/98/78

United Nations Educational Scientific and Cultural Organization
and
International Atomic Energy Agency

THE ABDUS SALAM INTERNATIONAL CENTRE FOR THEORETICAL PHYSICS

NUMERICAL STUDY OF THE SPIN-1 ASHKIN-TELLER MODEL

S. Bekhechi
Laboratoire de Magnétisme et de Physique des Hautes Energies,
Département de Physique, Faculté des Sciences, Universite Mohammed V,
Avenue Ibn Battota B.P. 10 14, Rabat, Morocco
and
The Abdus Salam International Centre for Theoretical Physics, Trieste, Italy

M. Badehdah, A. Benyoussef and B. Ettaki
Laboratoire de Magnétisme et de Physique des Hautes Energies,
Département de Physique, Faculté des Sciences, Universite Mohammed V,
Avenue Ibn Battota B.P. 10 14, Rabat, Morocco.

Abstract

Two non perturbative methods by means of the Transfer-Matrix Finite-Size-Scaling (TMFSS) and Monte-Carlo (MC) simulations are used to investigate the spin-1 Ashkin-Teller model (A.T.M). We have obtained rich phase diagrams with first and second order phase transitions with several multicritical points of higher order. Also this model exhibits a new partially ordered phase PO2 which does not exist in the spin-1/2 Ashkin-Teller model (A.T.M). Finally, the critical behaviour of this model is discussed.

MIRAMARE - TRIESTE

July 1998

I-Introduction:

The Ashkin-Teller model [1] (A.T.M.) is a generalisation of the Ising model to a four component systems. It may be considered as a superposition of two Ising models, which are described by variables σ_i and S_i sitting on each of the sites on a hypercubic lattice. Within each Ising model, there is a two spin nearest-neighbour interaction with strength K_2. In addition, the different Ising models are coupled by a four spin interaction with strength K_4. A good physical realisation for this model is the compound of Selenium adsorbed on N_i surface [2].

Different methods have been applied to study the critical behaviour of this model. For the two dimensional case, MFA and MC simulations [3], series analysis [4], exact duality [5], Transfer-Matrix calculations [2], renormalization group [6,7] and the mean-field renormalization group approach [8], have been applied. All these methods yield three different phases: Paramagnetic (P) phase in which neither σ nor S nor anything else is ordered ($<\sigma> = <S> = <\sigma S> = 0$); a Baxter phase in which σ and S independently order in a ferromagnetic fashion and also $<\sigma S>$ is unequal to zero and a third phase called PO1 in which σS is ordered ferromagnetically $<\sigma S>\neq 0$ but $<\sigma> = <S> = 0$. Apart from the variational approaches which give tricritical points, the other accurate methods yield only a line of critical points which connects the Ising critical point at one end to the four state Potts critical point at the other end, and along this line the exponents are varying continuously as confirmed recently by MC simulations using the cluster algorithm [9].

A new partially ordered phase where $<\sigma> \neq 0$ and $<S> = <\sigma S> = 0$ appears in the three dimensional antiferromagnetic A.T.M which has been studied by MFA and MC simulations [3]. By using exact duality transformations and symmetry considerations [10] the anisotropic A.T.M in d=2 presents also partially ordered phases called $<\sigma>$ and $<S>$ which are connected by symmetry operation to the $<\sigma S>$ phase. These results were confirmed recently in d=2 and d=3 by MFA and MC simulations [11].

Recently a spin-1 Ashkin-Teller model has been studied by using the effective field theory (EFT) [12]. The Hamiltonian of this model is:

$$H = -K_2 \sum_{\langle ij \rangle} \left(\sigma_i \sigma_j + S_i S_j \right) - K_4 \sum_{\langle ij \rangle} \sigma_i \sigma_j S_i S_j - D \sum_i \left(\sigma_i^2 + S_i^2 \right) \qquad (1)$$

where the spins σ_i and S_i are located on sites of an hypercubic lattice and take both the values ±1,0. The parameters $K_2 > 0$ and $K_4 > 0$ are respectively the two four spins interactions and there is on each site a single ion potential D. The phase diagrams obtained present a rich variety of phase transitions and for certain values of four coupling K_4, the anisotropy interaction D induces a new partially ordered phase called PO2 ($<\sigma>=<S> \neq 0$; $<\sigma S>=0$) which does not occur in the spin-1/2 Ashkin-Teller model.

The Finite-Size-Scaling theory based on Transfer-Matrix (TM) calculations and Monte-Carlo (MC) simulations, is a powerful and successful tool to study critical phenomena at reduced dimensionality (d=2). So, it is important to fully understand the phase diagram obtained from this model through nonperturbative methods such as Monte-Carlo and transfer-matrix techniques. The main problems which arise from these two methods are the increase of the size of the matrix (problems of diagonalization) with the strip width of the system for TMFSS calculations and statistical errors in MC simulations.

In this paper, we investigate the spin-1 Ashkin-Teller model using these two nonperturbative methods. We have obtained both phase diagrams and critical exponents for different values of parameters K_4 and D. The paper is organized as follows: In section II, we give the details of the transfer-matrix calculations and section III contains the Monte-Carlo simulations used to analyse this model. Section IV presents our results and a discussion. Finally in sec. V we draw our conclusion.

II-Transfer-matrix finite-size-scaling calculations:(TMFSS)

A detailed description of the phenomenological finite-size-scaling method and the transfer-matrix formalism on two dimensional systems are given in [2, 13, 14].

A system of linear size N is used with periodic boundary conditions, here only odd values of N are considered to avoid the introduction of interfaces and to preserve the ferromagnetic phases. With N'=N+1 the Nightingale condition [13] for the determination of the critical point K_C becomes:

$$\frac{\xi_N(K_c)}{N} = \frac{\xi_{N+1}(K_c)}{N+1} \tag{2}$$

where $\xi_N(K)$ is the correlation length. The symbol K denotes the set of fields K=(T, K_2, K_4, D). The nature of the transition (first-order or continuous) is determined by examining the finite-size-scaling behaviour of the persistence length $\tilde{\xi}$ [15, 16, 17, 18]. If the scaled persistence length $\tilde{\xi}/N$ on the transition line is a decreasing function of N then the transition is continuous, otherwise the transition is first-order.

The correlation length and the persistence length are obtained from the largest eigenvalues of the transfer-matrix. In the transfer matrix method, the lattice is approximated by an $2N\times\infty$ lattice (the number 2 arises because we have decomposed the ATM into adjacent layers where even (odd) layers contain σ (S) spins with a four spin interaction K_4) with periodic boundary conditions in the finite direction. The complete transfer matrix T(i,j) can be written as:

$$\begin{aligned}
&T(i,j) = T_1(\sigma_i,\sigma_j)T_2(s_i,s_j)T(\sigma_i s_i,\sigma_j s_j)\\
&T_1(\sigma_i,\sigma_j) = \mathrm{Exp}\left\{\frac{1}{T}\sum_{i=\mathrm{even}}^{2N}\left(K_2(\sigma_i\sigma_{i+1}+\sigma_i\sigma_j)+D\sigma_i^2\right)\right\}\\
&T_1(s_i,s_j) = \mathrm{Exp}\left\{\frac{1}{T}\sum_{i=\mathrm{odd}}^{2N}\left(K_2(s_i s_{i+1}+s_i s_j)+Ds_i^2\right)\right\}\\
&T_1(s_i\sigma_i,s_j\sigma_j) = \mathrm{Exp}\left\{\frac{K_4}{T}\sum_{i=1}^{2N}\left(s_i s_{i+2}\sigma_{i+1}\sigma_{i+3}+s_i s_j\sigma_{i+1}\sigma_{j+1}\right)\right\}
\end{aligned} \tag{3}$$

The full 9^N*9^N transfer matrix can be block diagonalized using invariance under the two step translation in the transverse direction. Since all phases are symmetric (ferromagnetic), the symmetric block, T^s (1665*1665 for N=4), is the only block whose symmetries correspond to ordered phases. We diagonalized it with RS library routines (based on EISPACK routines) on DEC stations 5000/200. The diagonalization results in four eigenvalues of interest. The largest eigenvalue of both T^s and the transfer matrix is λ_1^s. By virtue of the Perron-Frobenius theorem, it is positive and nondegenerate. The next three largest are λ_2^s, λ_3^s and λ_4^s. These four eigenvalues give rise to three important lengths:

$$\xi_1^s = \left(\ln\left|\lambda_1^s / \lambda_2^s\right|\right)^{-1} \tag{4}$$

is the largest length, it diverges exponentially with N in both ferromagnetic and PO2 phases.

$$\xi_2^s = \left(\ln\left|\lambda_1^s / \lambda_3^s\right|\right)^{-1} \tag{5}$$

is the second largest length, it diverges exponentially with N in both PO1 and ferromagnetic phases. And the persistence length corresponding to T^S is:

$$\xi_3^s = \left(\ln\left|\lambda_1^s / \lambda_4^s\right|\right)^{-1} \tag{6}$$

which remains small and peaks near the transition between ordered phases.

The correlation length exponent ν is obtained following the argument of Nightingale [13].

$$\nu^{-1} = Ln\left(\frac{N\partial\xi_N^{-1}(K_c)/\partial T}{(N+1)\partial\xi_{N+1}^{-1}(K_c)/\partial T}\right)\left(Ln(N/N+1)\right)^{-1} \tag{7}$$

III-Monte-Carlo simulation:

We have also performed Monte-Carlo simulations to complement transfer-matrix results. The system studied is L*L square lattice with even L, containing $N=L^2$ spins, and we use the well-known Metropolis algorithm [19] with periodic boundary conditions to update the lattice configurations. The physical quantities of use are the magnetizations $|M_\alpha|$ ($\alpha=\sigma$, S, σS) and are estimated by :

$$|M_\alpha| = \langle |M_\alpha| \rangle = \frac{1}{NS} \sum_c \sum_i \alpha_i(c) \qquad \text{with } \alpha = \sigma,\ S,\ \sigma S \tag{8}$$

where i runs over the lattice sites and c runs over the configurations obtained to update the lattice over one sweep of the entire N spins of the lattice (one Monte-Carlo step, MCS). The number of the MCS S is counted after the system reaches thermal equilibrium.

In order to measure the phase boundaries we shall find useful the measurement of fluctuations (variance of the order-parameter) in M_α defined by the magnetic susceptibility:

$$\chi_\alpha = \frac{N}{k_B T} \left(\langle M_\alpha^2 \rangle - \langle |M_\alpha| \rangle^2 \right) \qquad \text{with } \alpha = \sigma,\ S,\ \sigma S \tag{9}$$

IV- Results and discussion:

Our phase diagrams obtained by the Finite-Size-scaling theory from Monte-Carlo and transfer-matrix calculations, are shown in Figs. 1-3. The strip widths used for the TM are N/N'= 2/3 and 3/4. MC simulations were performed with systems of sizes L between 10 and 40. Most of the data were obtained with L=30 and 25 000 to 50 000 M.C.S after 5000 sweeps had been discarded for thermal equilibrium. First we discuss the limiting cases of this model:

- When the four coupling $K_4=0$, the Hamiltonian (1) is reduced to a two decoupled spin-1 Ising model: the Blume-Capel model where phase diagrams and critical behaviour have been extensively studied [20].

- For large positive crystal field ($D \to +\infty$), the state zero becomes unfavourable and the model is reduced to the usual spin-1/2 Ashkin-Teller model and for large negative, ($D \to -\infty$) we have a uniform ground state where all spins are zero.

a) <u>Phase diagrams</u>:

- For weak K_4, $K_4/K_2 = 1.0$, the phase diagram obtained by TMFSS and MC is shown in Fig. 1. We have only two phases: a paramagnetic (P) phase where $<\sigma> = <S> = <\sigma S> = 0$ and a ferromagnetic (F) (Baxter phase) phase where $<\sigma>$ and $<S>$ are ordered ferromagnetically and also $<\sigma S> \neq 0$. These two phases are separated by a critical line and first-order transition at high respectively low crystal field D/K_2. These two lines meet at a tricritical point C. The TMFSS results are obtained from the Nightingale criterion of the correlation length and for the strip of widths N/N' = 2/3 and 3/4, however the MC data are obtained from peaks in the susceptibilities for L = 30. The nature of the transition is determined from peaks in the persistence length for TMFSS and from discontinuities (continuities) and hysteresis behaviour in the order parameters for first (second) order transition by MC simulations [18] Figs. 2a-b. We also see in Fig. 1 that TM (3/4) and MC results are in excellent agreement with each other and qualitatively better than those obtained from EFT [12].

- When K_4/K_2 is increased, $K_4/K_2 > 1$, a new topology appears with new phases at high temperature and which do not exist at T = 0. Our results from TM and MC data are plotted in Fig. 3 for $K_4/K_2 = 4.0$. We have four phases: Paramagnetic and ferromagnetic phases and two new partially ordered phases called PO1 and PO2. The PO1 phase ($<\sigma> = <S> = 0$, $<\sigma S> \neq 0$, Fig. 4a.) appears at high anisotropy D/K2 and is the usual partially ordered phase of the spin-1/2 A.T.M. It separates the paramagnetic and ferromagnetic phases by lines of second-order. By decreasing the crystal field, a new PO2 phase ($<\sigma> = <S> \neq 0$, $<\sigma S> = 0$, Fig. 4b) appears at high temperature and separates the ferromagnetic phase from the paramagnetic phase by lines of second and first-order transitions. These lines meet at tricritical points. At low temperature, there is only a line of first-order separating the ferromagnetic phase from the paramagnetic phase Fig. 4c. In the phase diagram a multicritical point B^4 and a triple point A^3 at high respectively low temperature Also appear.

- To show the effect of strong K_4/K_2, we have also plotted in Fig. 5 phase diagram for K_4/K_2 = 6.0. All the phases remain and the only difference is a migration of the tricritical points to higher anisotropy values. We have also add 3/4 TM calculation to check the convergence of our data and with 2/3 scaling and MC results.

b) <u>Critical behaviour</u>:

The critical exponent ν is obtained from eq. 7 and the differentiation is made orthogonal to phase boundaries in order to have good estimates. Only results for K_4/K_2 = 1.0 and 6.0 are given, due to the use of strips of widths N/N' = 2/3 and 3/4. Since for N=2 the estimates of the critical temperature and the exponents are not very accurate and for N = 5 an entire block (of about 11817) of the transfer-matrix could not be stored in the available computers, we find it reasonable to stop here and no extrapolation of results is performed.

- For K_4/K_2 = 1, Fig. 6a shows the critical exponent ν for different values of D/K_2. For higher anisotropy the estimate of ν is 0.7192 with N/N' = 3/4 close to the four state Potts model $\nu = 2/3$ [21]. As discussed in the preceding section the model, for large D/K_2, is equivalent to the spin-1/2 A.T.M and for this value of K_4/K_2 = 1 this latter model lies in the four state Potts model [8, 9]. This value of ν still persists for low anisotropy until the tricritical point where ν_t decreases to 0.5557 which is in excellent agreement with the exact Ising tricritical exponent $\nu_t = 5/9$ [22, 23]. One of the main questions which arises here is whether the value of the tricritical exponent for K_4/K_2 = 1 belongs to the Ising tricritical universality or will lie to the four state Potts model where $\nu_t = 2/3$ [21]. So larger sizes are needed to confirm these results.

- For K_4/K_2 = 6 Fig. 6b, the estimates of ν with N/N' = 3/4 converge to the value 1 which is in very good agreement with the exact critical exponent ν= 1 [24, 25]. These results show that all critical lines are of Ising like critical points. At low anisotropy the estimates of ν decrease to ν_{t1} = 0.5613 and ν_{t2} = 05809, and are in good agreement with the known Ising tricritical exponent $\nu_t = 5/9$ [22, 23].

V- Conclusion:

We have made a thorough study of the spin-1 Ashkin-Teller model by using two non perturbative methods by means of transfer-matrix Finite-Size-Scaling calculations and Monte-Carlo simulations. Our results, obtained within these two exact numerical methods, are qualitatively better than those obtained with the effective Field theory. In the parameter space (K_4/K_2, D/K_2, T/K_2) the phase diagrams present rich varieties of phase transitions with surfaces of first and second-order transitions which are delimited by lines of tricritical, multicritical and triple points. It also appears for certain values of the four coupling K_4/K_2 and the anisotropy D/K_2, two partially ordered phases PO1 and PO2. The PO1 phase which exists in the spin-1/2 Ashkin-Teller model persists for spin-1 models, whereas the new PO2 phase does not exist in the usual spin-1/2 A.T.M. Also, the transfer-matrix Finite-Size-Scaling estimates of the exponent ν have shown that for $K_4/K_2 = 1$, we have a line of critical points which belong to the four states Potts model for a range of values of the anisotropy, instead of only one point of the four states Potts model in the spin-1/2 A.T.M. At lower D/K_2, the model falls into the Ising tricritical universality class. When the coupling K_4/K_2 becomes strong, $K_4/K_2 > 2$, the exponents calculations show that the critical lines separating the F-PO1 - P and F-PO2 - P phases belong to the Ising critical and triciritical universality classes. To confirm these results, larger sizes and powerful methods such as Monte-Carlo renormalisation are needed to have better estimates of the exponents and so to well define the universality of this simple but richer model.

Acknowledgements:

The authors thank D^r M. Loulidi, D^r A. Elkenz and D^r M. Touzani for discussions and criticisms. One of the authors, S. B thanks the Abdus Salam International Centre for Theoretical Physics (I.C.T.P), Trieste, Italy, for financial support and hospitality.

References:

[1]- J. Ashkin and E. Teller, Phys. Rev. **64**, 178 (1943)

[2]- P. Bak, P. Kleban, W.N. Unertel, J. Ochab, G. Akinci, N.C. Barlet and T. L. Einstein, Phys. Rev. Lett. **54**, 1542 (1985)

[3]- R. V. Ditzian, J. R. Banavar, G. S. Grest and L. P. Kadanoff, Phys. Rev. B **22**, 2542 (1980).

[4]- R. V. Ditzian, Phys. Lett A. **38**, 451 (1972)

[5]- F. J. Wegner, J. Phys. C. **5**, L 131 (1972)

[6]- J. R. Banavar, D. Jasnow and D.P Landau, Phys. Rev. B. **20**, 3820 (1979)

[7]- H. J. F. Knops, J. Phy A: Math. Gen. **8**, 1508 (1975).

[8]- J. A. Plascak and F.C Sà Barreto, J. Phy A: Math. Gen. **19**, 2195 (1986).

[9]- S. Wiesman and E. Domany, Phys. Rev. E. **48**, 4080 (1993); S. Wiesman and E. Domany, Phys. Rev E. **51**, 3074 (1994).

[10]- F. Y. Wu and K. Y. Lin, J. Phys. C **7**, L 181 (1974).

[11]- S. Bekhechi, A. Benyoussef, A. Elkenz, B. Ettaki and M. Loulidi, to appear in **Physica A.**

[12]- M. Loulidi, Phys. Rev. B **55**, 11611 (1997)

[13]- M. P. Nightingale, Physica A **83,** 561 (1976); Phys. Lett. A **59,** 486 (1977). M. P. Nightingale, J. Appl. Phys. **53,** 7927 (1982).

[14]- C. Domb, *Adv. Phys.* **9,** 149 (1960).

[15]- P. D. Beale, Phys. Rev. B **33,** 1717 (1986).

[16]- J. D. Kimel, P.A. Rikvold, and Y. L. Wang, Phys. Rev. B **45,** 7237 (1992).

[17]- P. A. Rikvold, W. Kinzel, J. D. Gunton, and K KASKI, *Phys. Rev. B* **28,** 2686 (1983).

[18]- S. Bekhechi and A. Benyoussef, Phys. Rev. B **56,** 13954 (1997).

[19]-"Applications of the Monte-Carlo Method in statistical physics" Edited by K.

Binder (1988).

[20]- M. Blume, Phys. Rev. **141**, 517 (1966).

- H. W. Capel, Physica (Amsterdam) **32**, 966 (1966); **33**, 295 (1967).

[21]- B. Nienhuis, in Phase Transition and Critical Phenomena, edited by C. Domb J. L. Lebowitz (Academic, New-York, 1987), Vol. 11.

[22]- M. P. M. denNijs, J. Phys. A **12**, 1857 (1979)

[23]- B. Nienhuis, E. K. Riedel and M. Schick, J. Phys. A **13**, L 189 (1980).

[24]- H. E. Stanley, Introduction To Phase Transitions and Critical Phenomena. (Oxford University Press, Oxford 1971).

[25]- B. M. McCoy and T. T. Wu, The Two dimensional Ising Model. (Harvard University Press, Cambridge, MA, 1973)

Figure captions:

- Fig. 1: The phase diagram in the D/K_2, T/K_2 plane for K_4/K_2=1.0, from Monte-Carlo (MC) and transfer-matrix (TM) data, is shown. TM results from 3/4 scaling (the 2/3 data are not shown for clarity) where × and Δ denote respectively second and first-order transitions. A tricritical point is located at (o) $C_{TM}(-2.3 \pm 0.1,\ 1.738 \pm 0.001)$ from 3/4 scaling. MC data are also shown with L=30 where + (◊) denote second (first) order transitions. The MC tricritical point is (□) $C_{MC}(-2.2 \pm 0.1,\ 1.82 \pm 0.01)$

-Fig. 2: Plot of order parameters $<\sigma>$, $<S>$ and $<\sigma S>$ versus T/K_2 for K_4/K_2=1 and different values of the anisotropy from MC simulations with L=30 show that there is only one transition. The corresponding inset shows associated susceptibilities.

a) D/K_2= 1.0, the three order parameters are continuous indicating that the transition is of second-order.

b) D/K_2= -2.5, the three order parameters are discontinuous indicating that the transition is of first-order.

- Fig. 3: The phase diagram in the D/K_2, T/K_2 plane for K_4/K_2=4.0, from Monte-Carlo (MC) and transfer-matrix (TM) data, is shown. The solid lines (first-order transition) and dashed lines (second-order transition) are the TM results from 2/3 scaling. Tricritical, multicritical and triple points are located respectively at $C_{TM}(-4.5 \pm 0.1,\ 3.4 \pm 0.001)$, $C'_{TM}(-4.4 \pm 0.01,\ 3.551 \pm 0.001)$, $B^4_{TM}(-3.5 \pm 0.1,\ 3.95 \pm 0.001)$ and $A^3_{TM}(-5.88 \pm 0.02,\ 1.8 \pm 0.1)$ from 2/3 scaling. MC data are also shown with L=30 where + (◊) denote second (first) order transitions. The MC tricritical, multicritical and triple points are located respectively at (□) $C_{MC}(-4.6 \pm 0.1,\ 3.35 \pm 0.01)$, (□) $C'_{MC}(-4.5 \pm 0.01,\ 3.62 \pm 0.01)$, $B^4_{MC}(-3.45 \pm 0.05,\ 4.08 \pm 0.01)$ and $A^3_{MC}(-5.85 \pm 0.02,\ 1.9 \pm 0.1)$.

- Fig. 4: Plot of order parameters $<\sigma>$, $<S>$ and $<\sigma S>$ for K_4/K_2=4 from MC simulations with L=30 in the neighbourhood of the multicritical point B^4, showing the existence of two new partially ordered phases at high temperature whereas at low temperature near the triple point A^3 there is only one transition. The corresponding inset shows associated susceptibilities.

a) D/K_2= -3.1, existence of the PO1 phase where at T_1= 4.23, <σ>=<S>=0 but <σS>≠ 0 whereas at T_2= 4.25 we have <σ>=<S>=<σS>= 0.

b) D/K_2= -3.9, existence of the PO2 phase where at $T_1^{'} = 3.91$, <S>=<σ>≠0 but <σS>=0 whereas at $T_2^{'} = 3.99$ we have <σ>=<S>=<σS>= 0.

c) T/K_2= 1.95, no partially ordered phases occur and the transition is first-order.

-Fig. 5: The phase diagram in the D/K_2, T/K_2 plane for K_4/K_2=6.0, from Monte-Carlo (MC) and transfer-matrix (TM) data, is shown. The solid lines (first-order transition) and dashed lines (second -order transition) are the TM results from 2/3 scaling. 3/4 results are also added to check convergence with 2/3 scaling and MC data, + and × denotes second and first-order transitions respectively. Tricritical, multicritical and triple points are located respectively at $C_{TM}(-6.4 \pm 0.1,\ 4.31 \pm 0.001)$, $C^{'}_{TM}(-6.4 \pm 0.01,\ 4.325 \pm 0.001)$, $B^{4}_{TM}(-6.25 \pm 0.05,\ 4.438 \pm 0.001)$ and $A^{3}_{TM}(-7.87 \pm 0.001,\ 2.3 \pm 0.1)$ from 2/3 scaling. MC data are also shown with L=30 where ◊ (Δ) denote second (first) order transitions. The MC tricritical, multicritical and triple points are located respectively at $C_{MC}(-6.4 \pm 0.1,\ 4.35 \pm 0.01)$, $C^{'}_{MC}(-6.45 \pm 0.05,\ 4.48 \pm 0.01)$, $B^{4}_{MC}(-6.1 \pm 0.1,\ 4.59 \pm 0.01)$ and $A^{3}_{MC}(-7.84 \pm 0.02,\ 2.42 \pm 0.02)$.

-Fig. 6: Estimates of the exponent ν versus D/K_2 for different values of K_4/K_2, as obtained by transfer-matrix calculations (see text for discussion) from N/N'=2/3 and 3/4 scaling.

a) K_4/K_2=1, (◊) from 2/3 scaling and (+) from 3/4 scaling. □ denotes the tricritical point from 3/4 scaling.

b) K_4/K_2=6, (+) from 2/3 scaling and (×) from 3/4 scaling for PO1-P and F-PO2 phase transitions, (1) is the associated tricritical point. Whereas (◊) from 2/3 scaling and (□) from 3/4 scaling for F-PO1 and PO2-P phase transitions, (2) denote the corresponding tricritical point.

Fig. 1

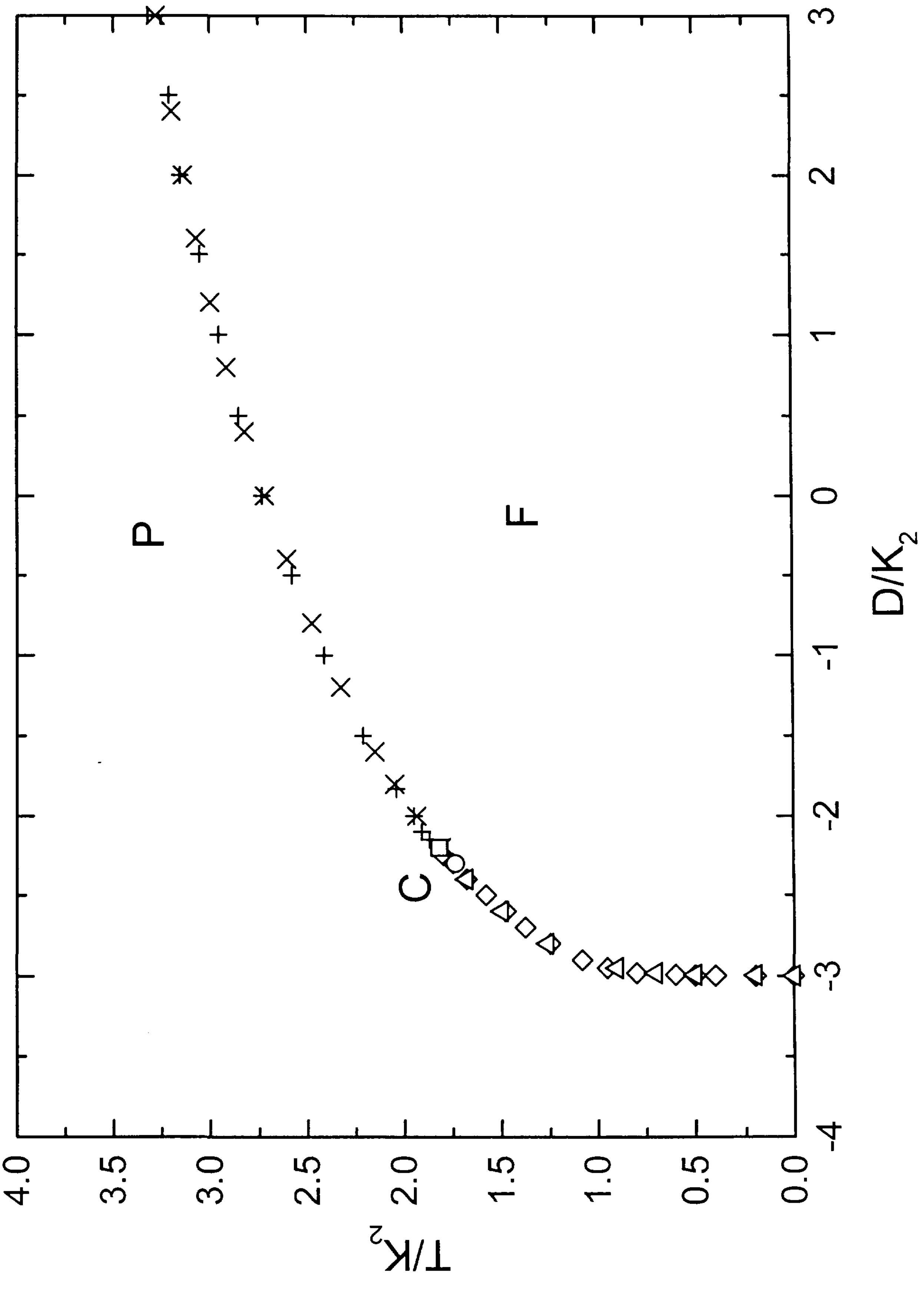

Fig. 2

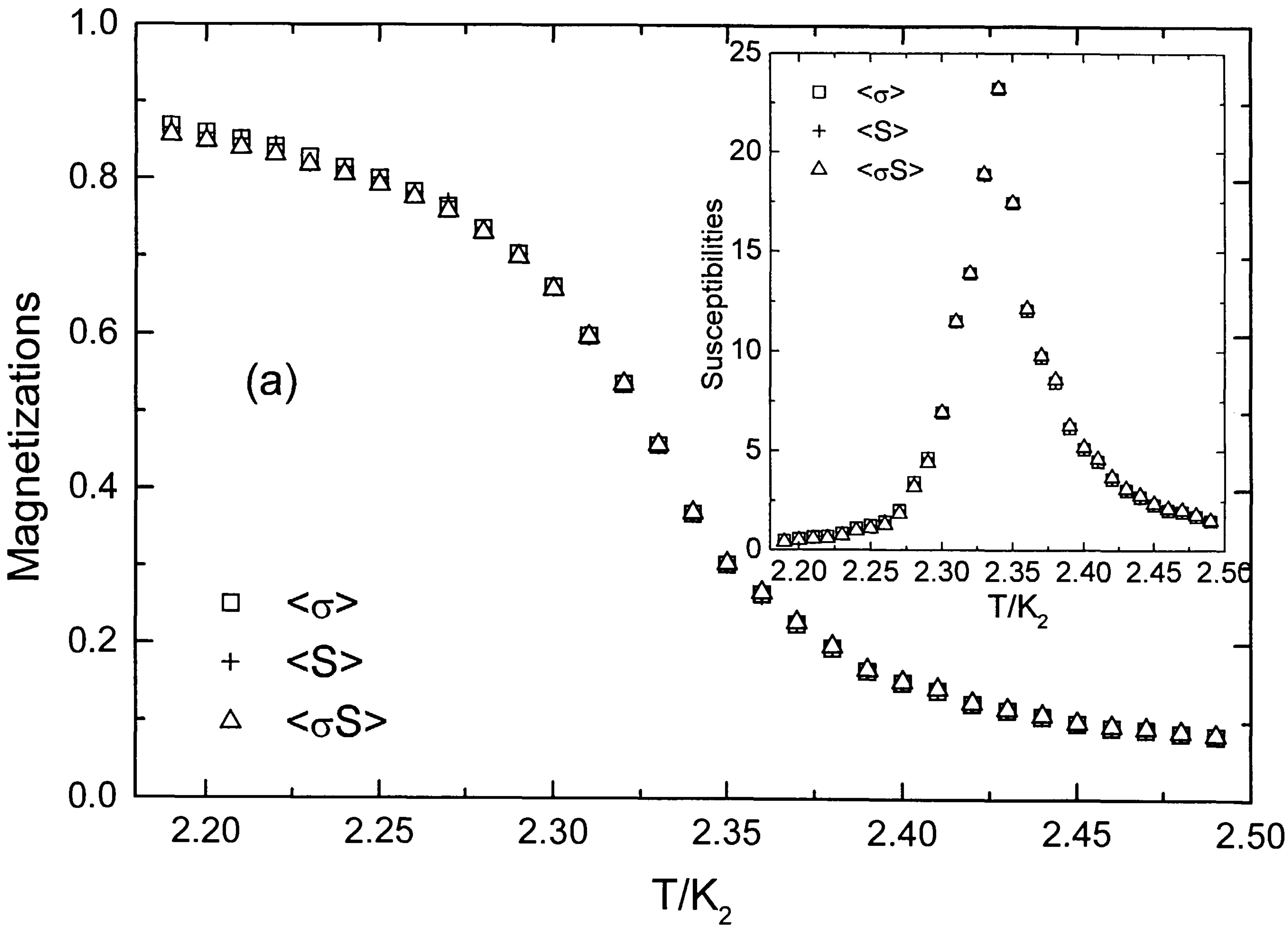

Magnetizations
1.0
0.8
0.6
0.4
0.2
0.0
2.20
2.25
2.30
2.35
2.40
2.45
2.50
T/K2
(a)
<σ>
<S>
<σS>
Susceptibilities
25
20
15
10
5
0
2.20 2.25 2.30 2.35 2.40 2.45 2.50
T/K2
<σ>
<S>
<σS>

Fig. 2

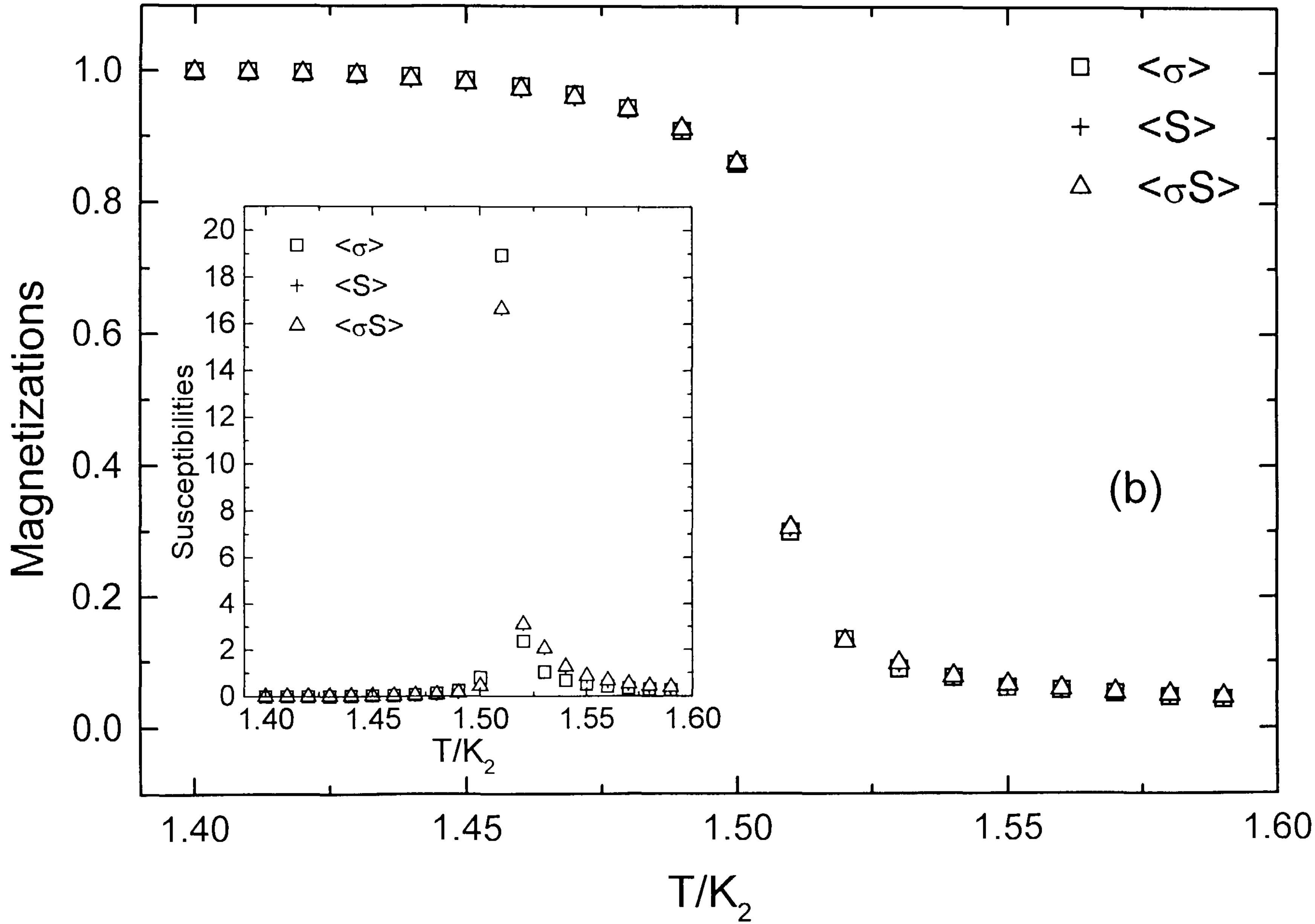

Magnetizations
1.0
0.8
0.6
0.4
0.2
0.0
1.40
1.45
1.50
1.55
1.60
T/K2
(b)
<σ>
<S>
<σS>
Susceptibilities
20
18
16
14
12
10
8
6
4
2
0

Fig. 3

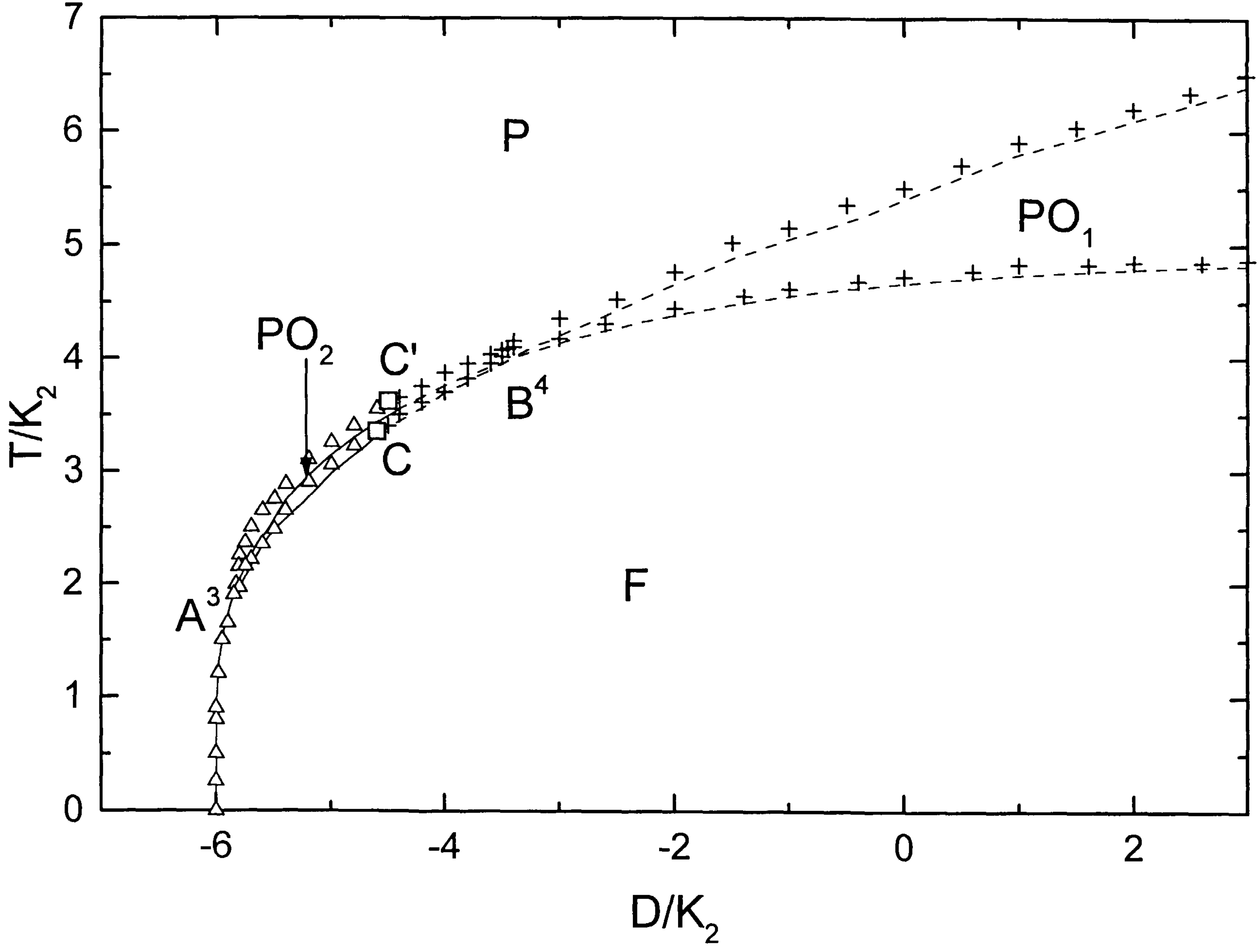

Fig. 4

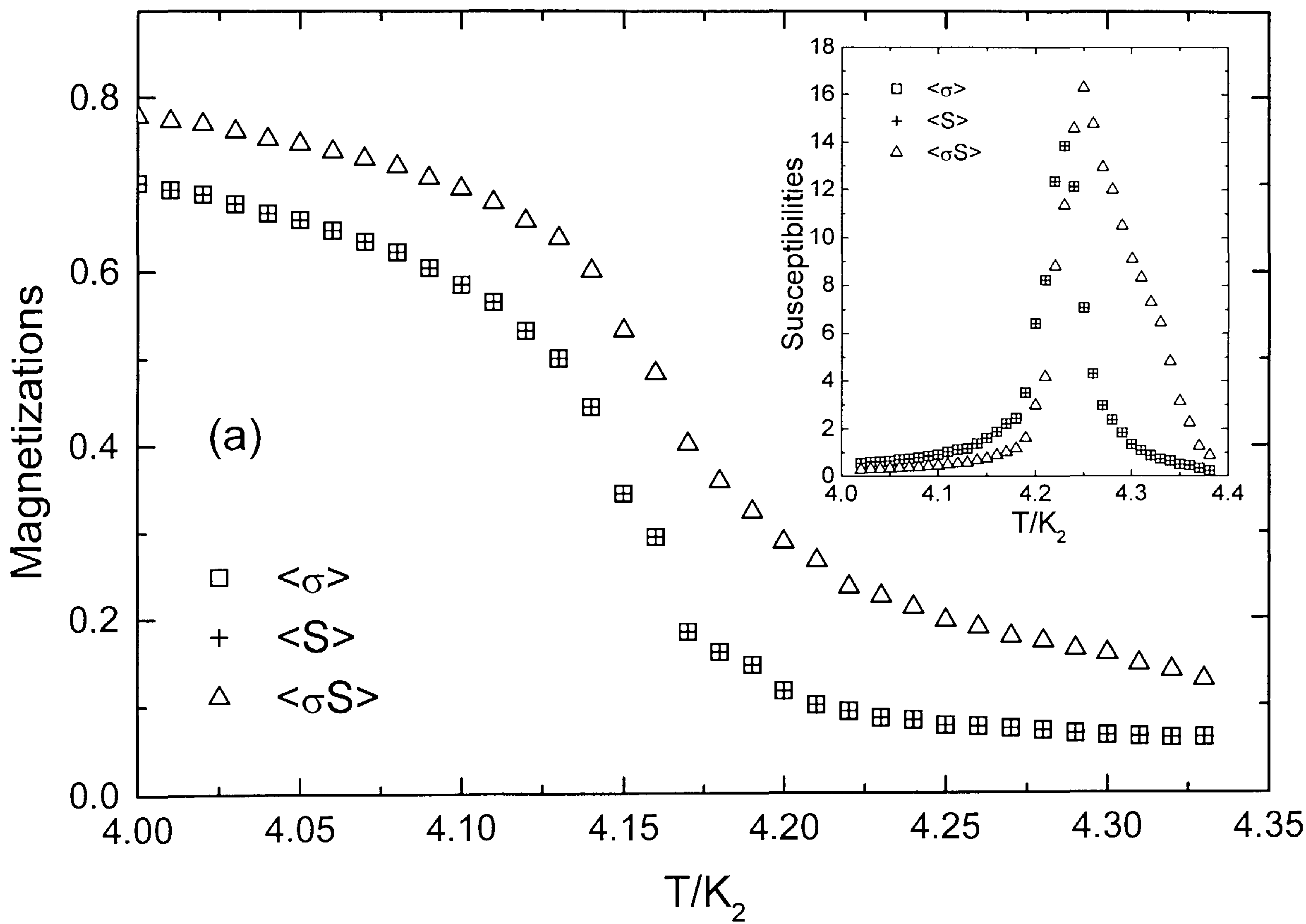

Fig. 4

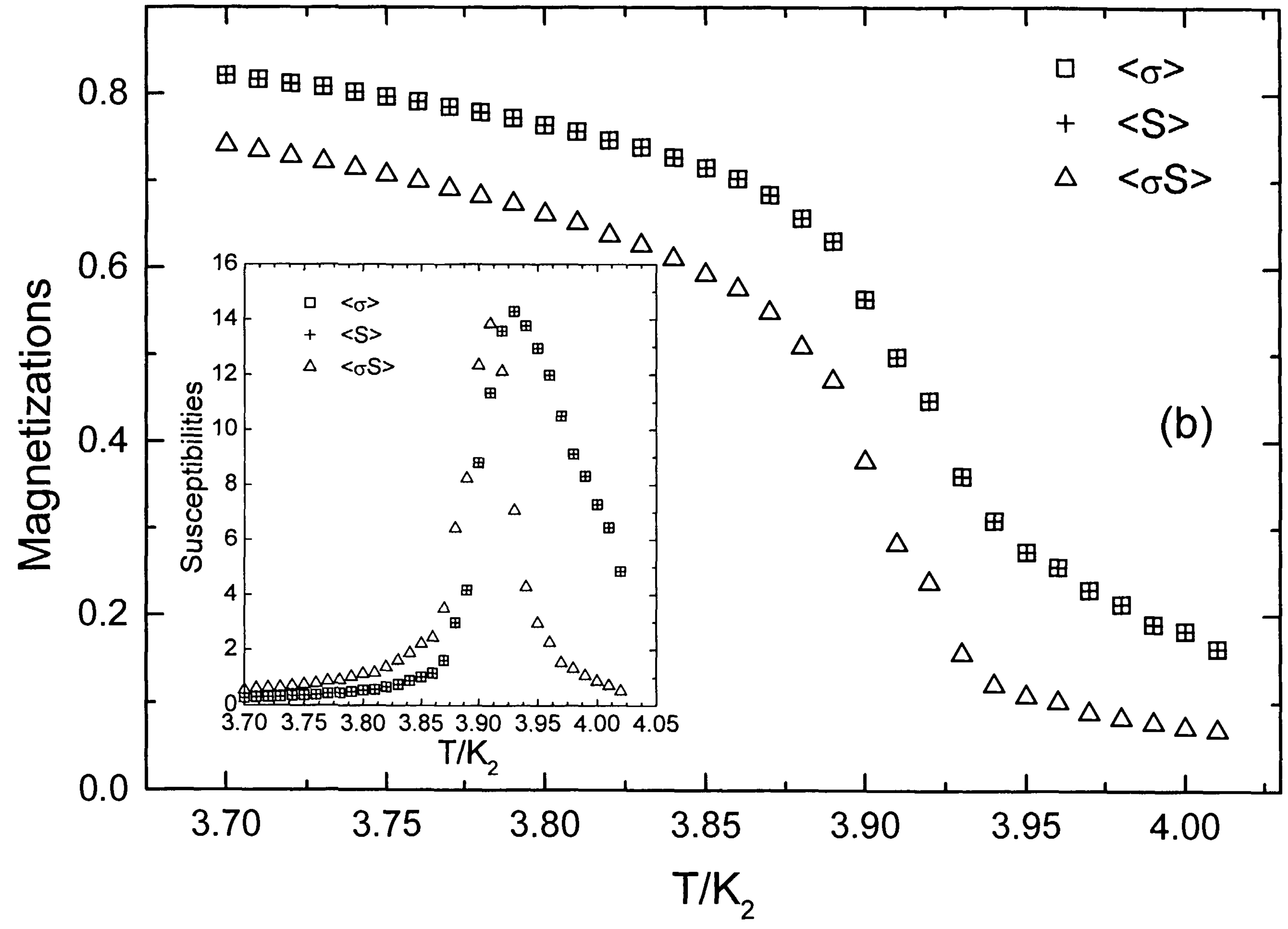

Fig. 4

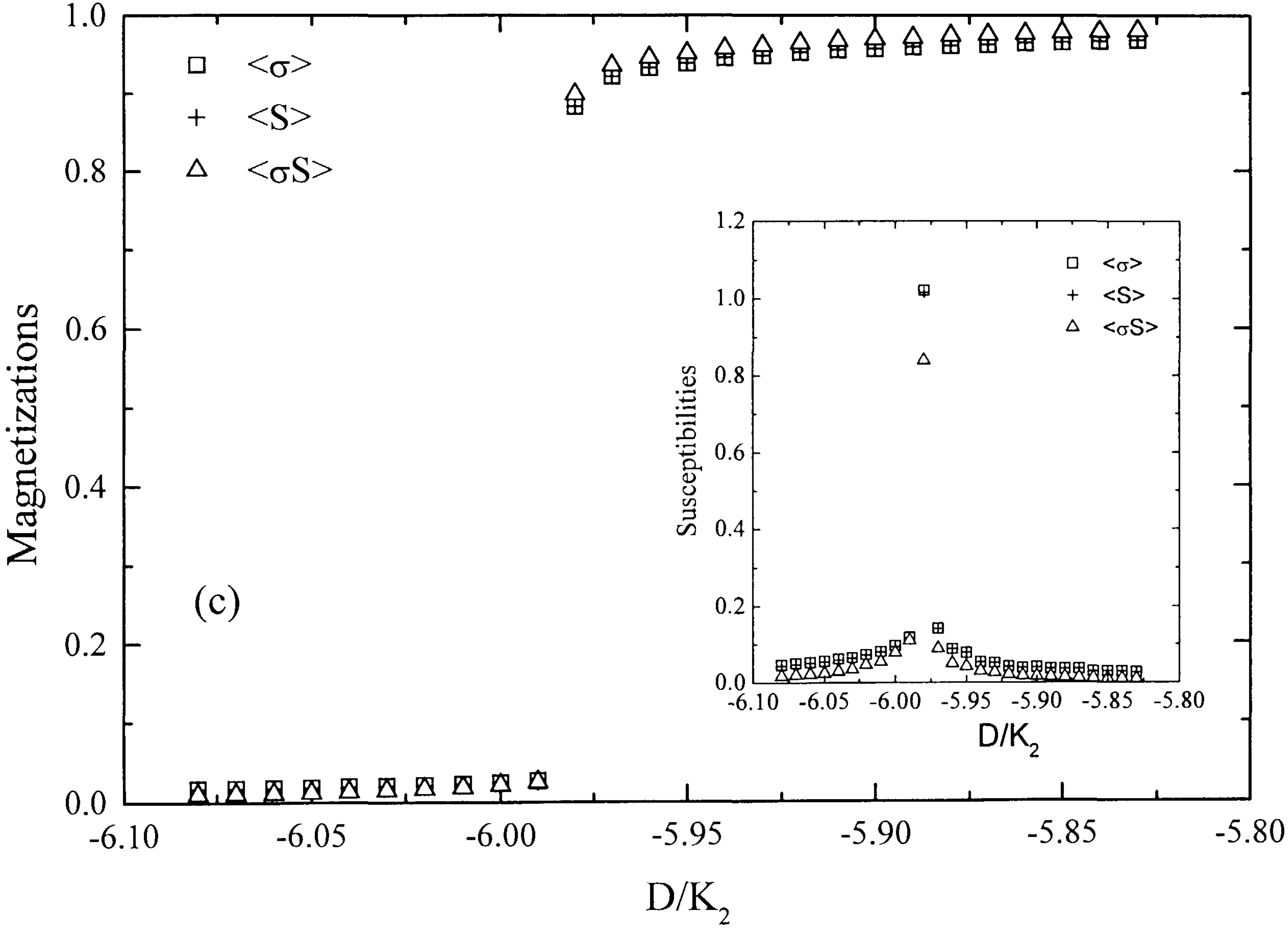

<σ>
<S>
<σS>
(c)
Magnetizations
D/K2
1.0
0.8
0.6
0.4
0.2
0.0
-6.10
-6.05
-6.00
-5.95
-5.90
-5.85
-5.80
Susceptibilities
1.2
<σ>
<S>
<σS>

Fig. 5

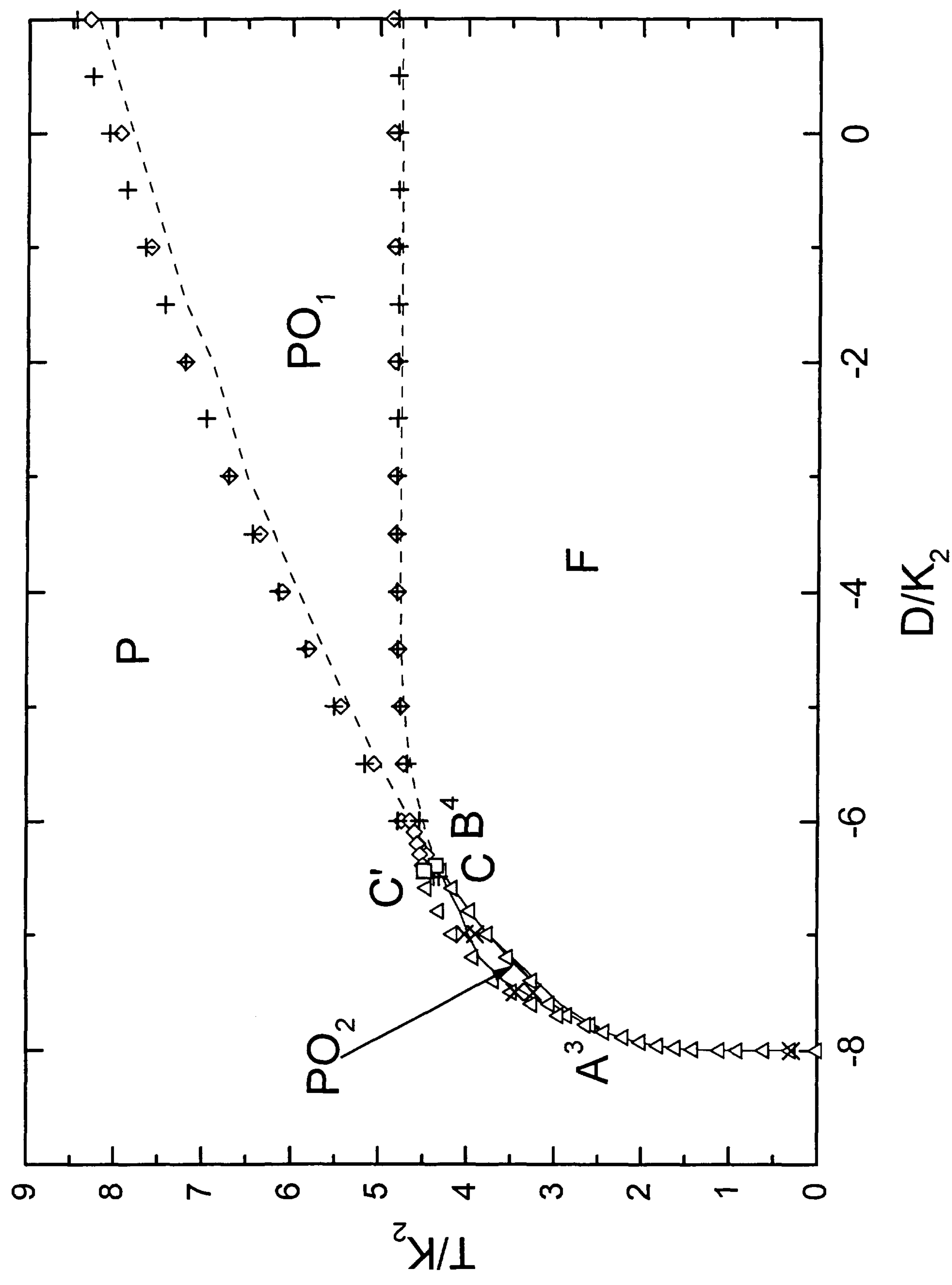

Fig. 6

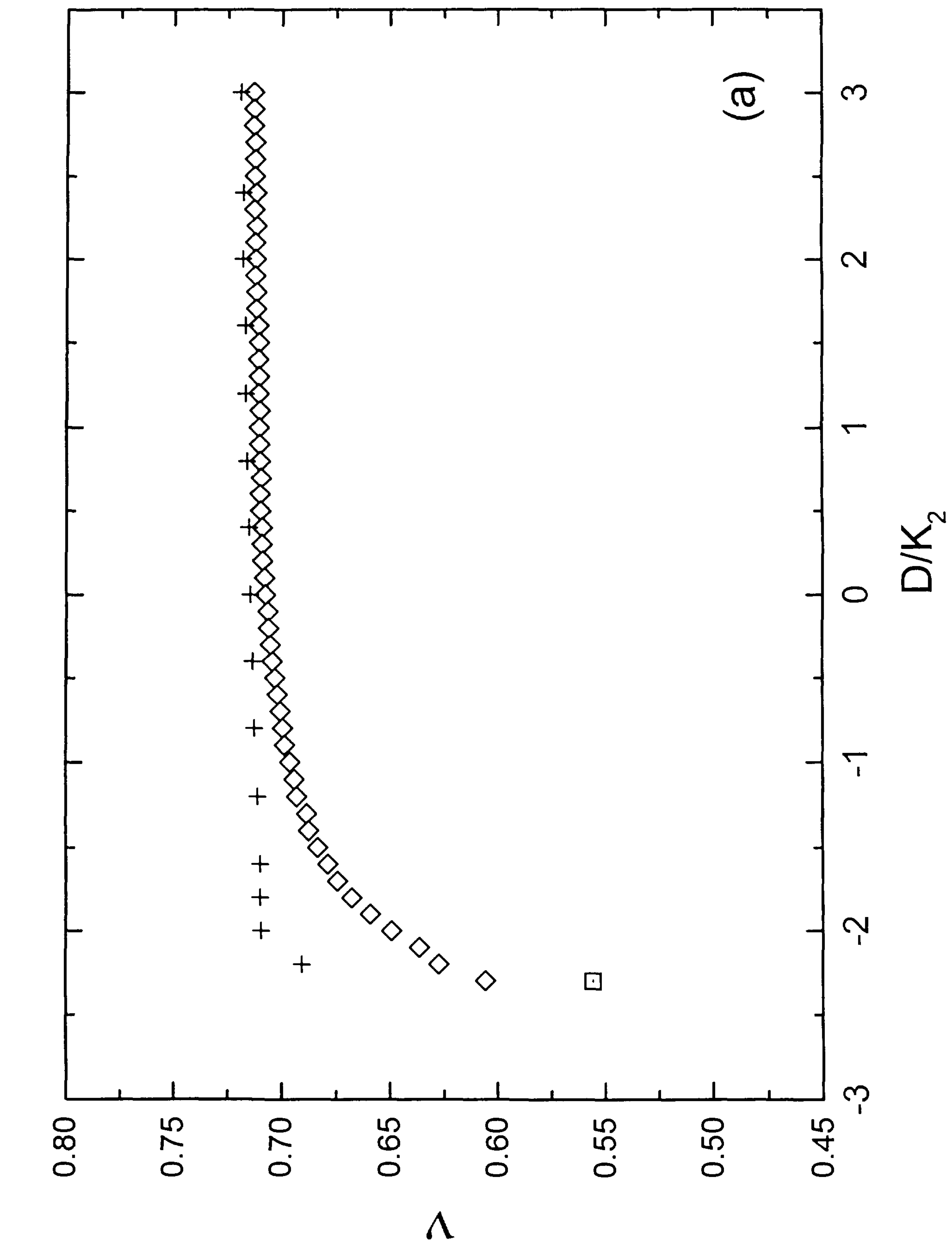

Fig. 6